Analysis of new actuation methods for capacitive shunt micro switchs

S Ben Sassi[1,a], M E Khater[2], E M Abdel-Rahman[3], and F Najar[1]

[1] Applied Mechanics and Systems Research Laboratory, Tunisia Polytechnic School, University of Carthage, B.P.743, La Marsa 2078, Tunisia
[2] Department of Mechanical Engineering, KFUPM, Dhahran, Saudi Arabia
[3] Department of Systems Design Engineering , University of Waterloo, Waterloo, ON, Canada

Abstract. This work investigates the use of new actuation methods in capacitive shunt micro switches. We formulate the coupled electromechanical problem by taking into account the fringing effects and nonlinearities due to mid-plane stretching. Static analysis is undertaken using the Differential Quadrature Method (DQM) to obtain the pull in voltage which is verified by means of the Finite Element Method (FEM). Based on Galerkin approximation, a single degree of freedom dynamic model is developed and limit-cycle solutions are calculated using the Finite Difference Method (FDM). In addition to the harmonic waveform signal, we apply novel actuation waveform signals to simulate the frequency-response. We show that, biased signals, using a square wave signal reduces significantly the pull-in voltage compared to the triangular and harmonic signal . Finally, these results are validated experimentally.

1 Introduction

MEMS technology is becoming an attractive technology thanks to an expanded applications domain and remarkable operational advantages [1,2]. RF MEMS switches are among the most important micro devices targeting a combination of high reliability and very low cost. Their role consists of performing circuit ON/OFF switching through a mechanical deflection. The driving force can be electrostatic, piezoelectric [3], electromagnetic [4] or a combination of them [5].

Electrostatic actuation is the most widespread method thanks to its simplicity and its near-zero power consumption. But a constant obstacle is the high actuation voltage required when designing MEMS switches. Reducing the pull-in voltage is essential not only for CMOS circuit integration but also to enhance the device lifetime. Researches have employed various methods to reduce the actuation voltage. Pacheco et al [6] designed a low-voltage RF MEMS switch by inserting folded suspensions above the micro beam. Balaraman et al [7] fabricated a low cost and actuation voltage RF micro switch using copper. Taking advantage of residual stress to induce buckling and bending, Chu et al [8] designed a high-isolation and low actuation voltage RF micro switch. Khater et al [9] demonstrated 60 % voltage reduction by changing the actuation mode from static to dynamic pull-in. Samaali et al [10] studied the dynamic behavior of a Single-Pole Double-Throw (SPDT) micro switch. They showed that the predicted pull in voltage using square signal is lower than that predicted for a harmonic wave.

In this work, we aim at studying the dynamic response of a micro switch under harmonic, square and triangular signal waveforms. Toward this end, we formulate the electromechanical problem of an electrostatic shunt micro switch.

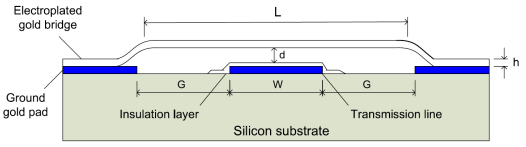

Fig. 1. A schematic diagram of the micro switch

We solve the static equation of equilibrium and calculate the static pull-in voltage using the Differential Quadrature Method (DQM). Then, we develop a Reduced Order Model (ROM) based on a one-mode Galerkin approximation and use the Finite Difference Method (FDM) to obtain the micro switch limit-cycles. Experimental tests are performed to validate the ROM. Finally, we study the impact of harmonic, square and triangle waveform signals on the micro switch numerically and experimentally and prove the superiority of square wave signal actuation.

2 Problem Formulation

The micro switch is one of the most popular devices in the telecommunications field. The switch under study is made of L long doubly-clamped micro beam fixed to a coplanar waveguide (CPW) as shown in Figure 1 [9]. The transmission line has a width W and is covered by a thin dielectric layer. Accounting for third order geometric nonlinearities and modeling the micro beam using the Euler-Bernoulli beam theory [11], the equation of motion that describes the beam deflection $\hat{w}(\hat{x},\hat{t})$ is given by:

$$\rho A\frac{\partial^2\hat{w}}{\partial\hat{t}^2}+(\hat{c}+\hat{c}_s)\frac{\partial\hat{w}}{\partial\hat{t}}+EI\frac{\partial^4\hat{w}}{\partial\hat{x}^4}=\frac{\varepsilon b_e V^2}{2(d-\hat{w})^2}S(\hat{x}) + \frac{\partial^2\hat{w}}{\partial\hat{x}^2}\Big[\hat{N}+\frac{EA}{2L}\int_0^L\Big(\frac{\partial\hat{w}}{\partial\hat{x}}\Big)^2dx\Big] \quad (1)$$

[a] e-mail: sara.bensassi@gmail.com

subject to two sets of fixed-end boundary conditions described by:

$$\hat{w}(0,\hat{t}) = \hat{w}(L,\hat{t}) = 0\,, \qquad \frac{\partial \hat{w}}{\partial \hat{x}}(0,\hat{t}) = \frac{\partial \hat{w}}{\partial \hat{x}}(L,\hat{t}) = 0 \quad (2)$$

Viscous damping is represented by $\hat{c} = \frac{\hat{\omega}}{Q}$ where $\hat{\omega}$ is the fundamental natural frequency of the micro switch and Q is its quality factor. Squeeze film damping is represented by [12]:

$$\hat{c}_s = \frac{\hat{\mu}\hat{b}^3}{(1+6K_n)(d-\hat{w})^3} \quad (3)$$

where $\hat{\mu}$ is air viscosity and K_n the Knudsen number. The axial force in the beam due to residual stresses is represented by $\hat{N}$ and ε is air permittivity.

The micro switch is actuated via the transmission line lying under the beam center only. In such a case, where the two 'electrodes' are not equal in length, it is important the fringing electrostatic field must be taken into account when evaluating the electrostatic force [13]. To represent the non-overlapping lower electrode (transmission line), we adopt the function $S(\hat{x})$ given by:

$$S(\hat{x}) = \begin{cases} 1 \text{ if } G \le \hat{x} \le L-G \\ 0 \quad \text{elsewhere} \end{cases} \quad (4)$$

The effects of the fringing field are taken into account through the deployment of an effective beam width b_e [12]:

$$b_e = (1 + 0.65\frac{d-\hat{w}}{b})\hat{b} \quad (5)$$

For convenience in implementation of DQM discretization, we rewrite Equations (1) and (2) in non-dimensional form as:

$$\frac{\partial^2 w}{\partial t^2} + (c+c_s)\frac{\partial w}{\partial t} + \frac{\partial^4 w}{\partial x^4} = \frac{\partial^2 w}{\partial x^2}\Big[N + \alpha_1 \int_0^1 \Big(\frac{\partial w}{\partial x}\Big)^2 dx\Big] + \alpha_2 \frac{V^2}{(1-w)^2}\Big(1 + 0.65\frac{1-w}{b}\Big)S(x) \quad (6)$$

subject to the boundary conditions:

$$w(0,t) = w(1,t) = 0\,, \qquad \frac{\partial w}{\partial x}(0,t) = \frac{\partial w}{\partial x}(1,t) = 0 \quad (7)$$

where:

$$x = \frac{\hat{x}}{L},\ w = \frac{\hat{w}}{d},\ t = \frac{\hat{t}}{T},\ \omega = \frac{\hat{\omega}}{T},\ b = \frac{\hat{b}}{d}$$
$$c = \frac{\hat{c}L^4}{EIT},\ c_s = \frac{\mu}{(1+6K_n)(1-w)^3},\ \mu = \frac{\hat{\mu}\hat{b}^3L^4}{EIT}, \quad (8)$$
$$\alpha_1 = 6\frac{d^2}{h^2},\ \alpha_2 = \frac{6\varepsilon L^4}{Eh^3d^3},\ N = \frac{\hat{N}L^2}{EI}$$

3 Static Response and Pull-in Voltage

The first step in studying of the micro switch is to determine its static response and predict its pull in voltage, which defines the actuation limit for electrostatic MEMS. To this end, we employ the DQM which consists of discretizing the domain using nonuniform grid points, then expressing the displacement function (beam deflection) and its derivatives as weighted linear combinations of the beam displacement at the grid nodes. We adopt the Chebyshev-Gauss-Lobatto grid distribution scheme thanks to its accuracy compared to grid distributions [14]. The derivatives of the displacement function are then approximated by:

$$\Big[\frac{\partial w^r(x)}{\partial x^r}\Big]_{x=x_i} = \sum_{j=1}^{n} A_{ij}^{(r)} w_j \quad (9)$$

Where the weighting coefficients are determined using the Lagrange interpolation polynomials. They are given by:

$$A_{ij}^{(1)} = \frac{\prod_{v=1;v\neq i}^{n}(x_i - x_v)}{(x_i-x_j)\prod_{v=1;v\neq j}^{n}(x_j-x_v)},\quad i,j = 1,2,...,n, j\neq i \quad (10)$$

$$A_{ij}^{(r)} = r\Big(A_{ij}^{r-1}A_{ij}^{1} - \frac{A_{ij}^{r-1}}{(x_i-x_j)}\Big),\quad i,j = 1,2,...,n; j\neq i \quad (11)$$

$$A_{ij}^{(r)} = -\sum_{v=1;v\neq i}^{n} A_{iv}^{(r)},\quad i = j = 1,2,...,n \quad (12)$$

Due to non-overlapping of the micro structure capacitor plates, two of the grid points must correspond to the edges of the lower electrode. To achieve that, we discretize the beam into 49 nodes. The micro switch dimensions are: $L = 225\,\mu m$, $\hat{b} = 20\,\mu m$, and $h = 1.7\,\mu m$. The initial capacitor gap is $d = 1.7\,\mu m$. It is fabricated from polysilicon with material properties $E = 80\,\text{GPa}$ and $\rho = 9320\,\text{kg/m}^3$ and residual stress of $\sigma = 17\,\text{GPa}$.

In addition to solving the static version of Equation (6) using the DQM, we performed a FEM analysis of the micro switch using the commercial software ANSYS. We compare the FEM results to those of the DQM to validate it. Table 1 shows the calculated static pull-in voltage using DQM, FEM and published results for the same micro switch in [9]. The comparison shows good agreement between DQM and FEM despite the large number of grid points.

Table 1. Comparison of static pull-in voltage values

DQM	FEM	Experiment [9]
64 *V*	66.45 *V*	68.5 *V*

4 Dynamic Response of the Micro Switch

To solve the equation of motion, Equation 6, we utilize an innovative ROM based on Galerkin decomposition and FDM. The novelty in this method is to adopt a discretized mode shape calculated using 49 grid points in the DQM [15]. We take advantage of the discretized mode shape $\phi(x_i)$ in the Galerkin approximation of the equation of motion. This allows us to reduce the number of modes retained in the Galerkin expansion and therefore, to reduce considerably the computational time of simulations.

Writing the dynamic displacement as

$$w(x,t) = q(t)\phi(x)$$

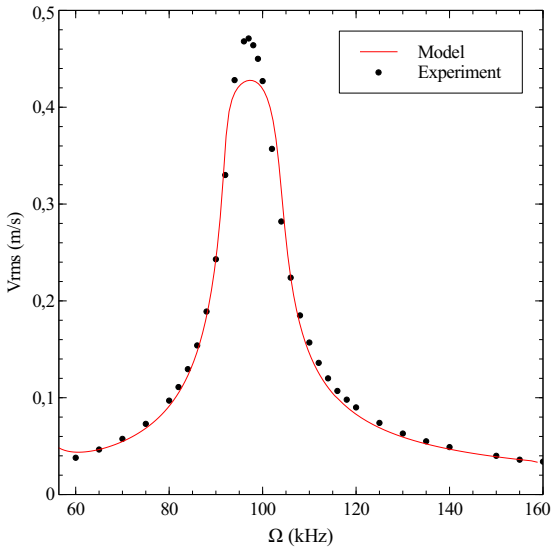

Fig. 2. Frequency-response curves of the micro switch mid-point velocity when actuated by a harmonic signal with $V_{dc} = 23\ V$, $V_{ac} = 23.28\ V$

where $q(t)$ is the modal coordinate and integrating the resulting equation using Newton-Cotes rule, we end up with the following reduced order model:

$$\begin{aligned}&\ddot{q} + \dot{q}(c + c_s) + q\sum_{i=1}^{n} C_i\phi_i \sum_{j=1}^{n} A_{ij}^{(4)}\phi_j \\ &+ \alpha_1 q^3 \sum_{i=1}^{n} C_i\phi_i \sum_{j=1}^{n} A_{ij}^{(2)}\phi_j \sum_{k=1}^{n} C_k\phi_k \sum_{v=1}^{n} A_{kv}^{(2)}\phi_v \\ &- Nq\sum_{i=1}^{n} C_i\phi_i \sum_{j=1}^{n} A_{ij}^{(2)}\phi_j = \alpha_2\Big(\sum_{i=1}^{n} C_i\phi_i \frac{V^2}{(1-q\phi_i)^2}\Big) \\ &\times\Big(1 + 0.65\frac{(1-q\phi_i)}{b/d}\Big)S_i\end{aligned} \tag{13}$$

where we write $\phi_i = \phi(x_i)$, the approximate value of the cord length integral is given by:

$$C_i = \int_0^1 \prod_{v=1;v\neq i}^{n} \frac{x-\zeta_v}{\zeta_i-\zeta_v}dx \tag{14}$$

and ζ_v are the grid points used in the DQM. The function:

$$S_i = \begin{cases} 1 & \frac{n+1}{2} - 4 \le i \le \frac{n+1}{2} + 4 \\ 0 & \text{elsewhere} \end{cases} \tag{15}$$

is a discretized unit-step function representing the size of the lower electrode compared to the micro switch span. We use a two-step finite difference scheme to rewrite the time derivatives in Equation (13) and 150 time steps to decompose one orbit. The resulting linear algebraic system is then solved to obtain the limit cycle corresponding to the operating conditions.

To investigate the validity of the proposed ROM, we perform experiments on the shunt micro switch using a harmonic signal in the form:

$$V(t) = 23 + 23.28\cos(\Omega t)\ (\text{V})$$

Figure 2 displays good agreement between the micro switch frequency-response curves of the midpoint RMS velocity

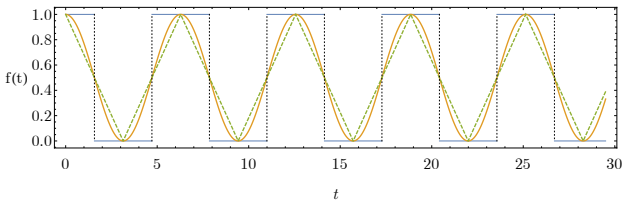

Fig. 3. Actuation waveforms: square (solid thin), harmonic (solid thick) and triangular (dashed)

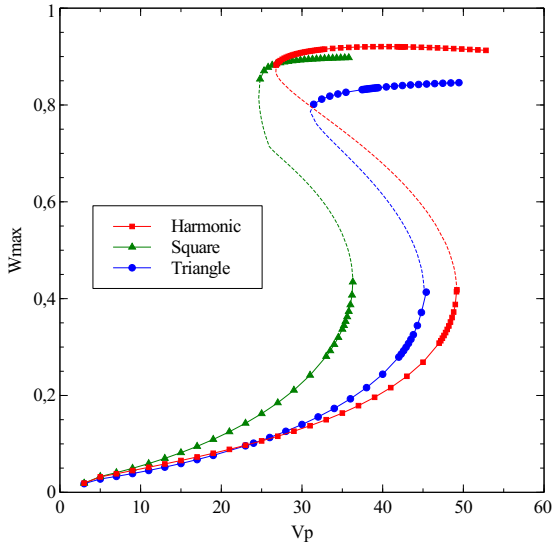

Fig. 4. The force-response curves under square (green), harmonic (red) and triangular (blue) actuation waveforms

obtained from the ROM and the experiment. We conclude that adopting a one-mode approximation is enough to converge to the solution.

Next, we compare among the dynamic response of the micro switch under the three biased square, harmonic, and triangular waveforms plotted in Figure 3. The normalized maximum (mid-point) deflection of the micro switch is shown in Figure 4 as a function of the peak voltage V_p of the harmonic, square and triangular voltage signals for $\Omega = 70\,kHz$. The bias voltage is set to $V_{DC} = 20V$ for all three signals. In each case, dynamic pull in occurs due to a homoclinic bifurcation observable in the phase space.

We remark that the lowest dynamic pull-in voltage is attained at $V_p = 20 + 36.3\,g(\Omega t)$ using the square function $g(t)$ while the highest one is attained at $V_p = 20 + 49.2\cos(\Omega t)$ for a harmonic signal. The dynamic pull-in for triangular signals expressed mathematically by the function $h(t)$ is obtained at $V_p = 20 + 45.2\,h(\Omega t)$. We conclude that a square actuation voltage signal is a more efficient approach to the actuation of micro switches than harmonic or triangular waveforms since it reduces considerably the dynamic pull in voltage required to switch the state of (open and close) MEMS shunt switches.

5 Conclusion

In this work, we carried out numerical and experimental studies of a shunt micro switch. First, we studied the static response of the micro switch under DC voltage using the DQM to solve the equation of equilibrium. We validated

our model by comparing the predicted static pull-in voltage to that predicted using an FEM model and previous experimental results. Then, we built a ROM based on one-term modal decomposition and FDM to obtain the limit-cycle of the micro switch for three waveforms: harmonic, square, and triangular. Comparison of simulations and experimental findings shows good agreement and validates our model. Besides this, we demonstrate that the micro switch responds differently to the three signals. In fact, it was shown that for a biased signals, a square waveform reduces considerably the actuation voltage compared with harmonic and triangular waveforms. This is an important insight in the design of low voltage MEMS shunt switches.

References

1. Yadav, R., Yadav, R., Nehra, V., & Rangara, K. J. Key Features, Application & Design Tools.
2. KOBAYASHI, S., & KAWAI, H. (2004). A Capacitive RF MEMS Shunt Switch. In International Workshop on SiP/SoC Integration of MEMS and Passive Components with RF-ICs, Chiba.
3. Park, J. H., Lee, H. C., Park, Y. H., Kim, Y. D., Ji, C. H., Bu, J., & Nam, H. J. (2006). A fully wafer-level packaged RF MEMS switch with low actuation voltage using a piezoelectric actuator. Journal of Micromechanics and Microengineering, 16(11), 2281.
4. Gatzen, H. H. (2012, June). Magnetic micro and nano actuator systems. In Meeting Abstracts (No. 48, pp. 3409-3409). The Electrochemical Society.
5. Bahrami, M. N., Yousefi-Koma, A., & Raeisifard, H. (2014). Modeling and nonlinear analysis of a micro-switch under electrostatic and piezoelectric excitations with curvature and piezoelectric nonlinearities. Journal of Mechanical Science and Technology, 28(1), 263-272.
6. Pacheco, S. P., Katehi, L. P., & Nguyen, C. C. (2000, June). Design of low actuation voltage RF MEMS switch. In Microwave Symposium Digest. 2000 IEEE MTT-S International (Vol. 1, pp. 165-168). IEEE.
7. Balaraman, D., Bhattacharya, S. K., Ayazi, F., & Papapolymerou, J. (2002, June). Low-cost low actuation voltage copper RF MEMS switches. In Microwave Symposium Digest, 2002 IEEE MTT-S International (Vol. 2, pp. 1225-1228). IEEE.
8. Chu, C. H., Shih, W. P., Chung, S. Y., Tsai, H. C., Shing, T. K., & Chang, P. Z. (2007). A low actuation voltage electrostatic actuator for RF MEMS switch applications. Journal of micromechanics and microengineering, 17(8), 1649.
9. Khater, M. E., Vummidi, K., Abdel-Rahman, E. M., Nayfeh, A. H., & Raman, S. (2011). Dynamic actuation methods for capacitive MEMS shunt switches. Journal of Micromechanics and Microengineering, 21(3), 035009.
10. Samaali, H., Najar, F., Ouni, B., & Choura, S. (2015). MEMS SPDT microswitch with low actuation voltage for RF applications. Microelectronics International, 32(2), 55-62.
11. Younis, M. I. (2011). MEMS linear and nonlinear statics and dynamics (Vol. 20). Springer Science & Business Media.
12. Osterberg, P. M., & Senturia, S. D. (1997). M-TEST: a test chip for MEMS material property measurement using electrostatically actuated test structures. Microelectromechanical Systems, Journal of, 6(2), 107-118.
13. Snow, M. G., & Bajaj, A. K. (2015). Uncertainty quantification analysis of the dynamics of an electrostatically actuated microelectromechanical switch model. Journal of Sound and Vibration, 349, 375-388.
14. Bert, C. W., & Malik, M. (1996). Differential quadrature method in computational mechanics: a review. Applied Mechanics Reviews, 49(1), 1-28.
15. Sassi, S. B., & Najar, F. (2015). Novel Reduced Order Model for Electrically Actuated Microbeam-Based MEMS. In Design and Modeling of Mechanical Systems-II (pp. 513-520). Springer International Publishing.